Autogenous healing in ultra-high-performance fibre reinforced concrete: application in two reduced scale water reservoirs

Marta Caballero-Jorna[1,*], *Hesam* Doostkami[1], *Marta* Roig-Flores[2], and *Pedro* Serna[1]

[1] Universitat Politècnica de València, Instituto de Ciencia y Tecnología del Hormigón, Valencia, Spain
[2] Universitat Jaume I, Departamento de Ingeniería Mecánica y Construcción, Castellón de la Plana, Spain

Abstract. Self-healing is defined as the capacity of a material to repair internal damage without any external intervention. In the case of concrete, this process can be autogenous, which is the natural capacity of the material. Ultra-High-Performance Fibre Reinforced Concrete (UHPFRC) has a high self-healing potential due to its high binder content with a low w/b ratio and its crack pattern with multiple micro cracks. This paper describes two UHPFRC water reservoirs, which were designed to minimise the volume of concrete used. The design is made of ribbed thin walls where shrinkage cracks are likely to happen. The objective of this work is to study the autogenous healing capability of this concrete in these cracks. The two water reservoirs have internal dimensions of 1.30×0.75×0.70 m³ and with 20 mm thickness in the centre of the walls. These walls displayed cracks (w < 100 μm), which were produced just after casting. Both reservoirs were filled with water, showing apparent water leakage. The cracks were monitored for 30 days, analysing pictures taken with an optical microscope. The results show that UHPFRC is able to heal autogenously under the conditions in this work, recovering completely the water tightness required for the water reservoirs.

Keywords: autogenous healing, case study, permeability, shrinkage, Ultra High-Performance Fibre Reinforced Concrete, water leakage.

1 Introduction

Current design practices for water reservoir structures are based on using additional steel reinforcement to effectively control cracking [1].

EN1992-Part 3 [2] includes indications for the design of liquid retaining and containment structures, constructed from plain or lightly reinforced concrete, reinforced concrete, or prestressed concrete. When considering the serviceability limit state of cracking, this code includes different requirements classifying the structures with different tightness classes. These classes depend on the degree of leakage that is acceptable. For class 0 structures, some degree of leakage is acceptable (*e.g.* for the storage of dry materials). Class 1 structures may have some small leakage and some surface staining or damp patches are acceptable. Class 1 structures limit the characteristic crack width (w_{k1}) expected to pass through the full thickness. For class 2, leakage must be minimal, and appearance must not be impaired by cracks and, for class 3, no leakage is permitted. In classes 2 and 3, cracks should not pass through the full width of a section.

In class 1 structures, the recommended limit for the characteristic crack width is defined as a function of the ratio of the hydrostatic pressure (h_D) to the wall thickness of the containing structure (h). The code indicates that for ratios $h_D/h \leq 5$, crack width w_{k1} should be limited to 0.2 mm while for $h_D/h \geq 35$, w_{k1} should be limited to 0.05 mm, and that for intermediate values of the h_D/h ratio, w_{k1} can be interpolated. Any crack with a width below these values, is expected to have an effective sealing within a relatively short time. Another relevant indication is that in the absence of more reliable information, sealing may be assumed where the expected strain under service conditions is below 150×10^{-6} (0.15‰). For conditions where self-healing is unlikely, any crack which passes through the full thickness of the section may lead to leakage, regardless of its width.

FRCs can be an advantageous material in water-retaining structures due to their cracking reduction, mainly due to the reduction of shrinkage, flexural cracking, and structural deformation [1], [3], which leads to a more watertight structure. Ultra-High-Performance Fibre Reinforced Concrete (UHPFRC) can be even more advantageous material to ensure watertightness. UHPFRC is a fibre-reinforced concrete that presents a high mechanical performance (high ductility, high strength) and improved durability (low permeability, crack pattern with multiple micro cracks) compared with conventional concretes [4]. UPHFRC is characterised by a high amount of binder, small aggregates, low water-to-binder (w/b) ratio, and high volumes of fibres.

* Corresponding author: marcajor@upv.es

There are some concerns regarding UHPC and UHPFRC shrinkage due to their high binder content and low w/b ratio; however, their response is different for autogenous and drying shrinkage [5]. Autogenous shrinkage is produced by hydration, and in UHPC and UHPFRC it is expected to be large due to their low water content [5]. Several studies have reported moderate or high autogenous shrinkages in UHPC and UHPFRC [5]–[7]. Drying shrinkage is a time-dependent deformation produced at constant temperature, which is higher for mixes with high water contents, thus, in UHPC and UHPFRC it will be lower than in conventional concrete [5]. The addition of fibres to UHPC has been reported to reduce both, autogenous [8] and drying shrinkage [9], and therefore, it will reduce the potential early-age cracking of the mix.

The presence of cracks may compromise the durability of concrete and reinforcement and thus, reduce the retaining structures' functionality. However, due to UHPFRC's extremely dense matrix, with a very low amount of capillary pores, and its cracking pattern with very tight cracks, this material is practically impermeable for liquids, even under high tensile strains up to about 1.5 ‰ [10], and with reduced availability of oxygen even at those strain levels [11]. In addition, UHPFRC displays relevant self-healing properties [12]–[15] showing that its healed cracks are able to recover some mechanical properties, to recover water tightness, and to recover protection potential against the penetration of chlorides.

Various studies have analysed cracking in water reservoir structures made with reinforced concrete. There are few experimental works performed on UHPFRC prototypes as retaining or water retaining structures.

One study [16] analysed full-scale experimental cantilever retaining walls made with reinforced UHPFRC, testing different fibre volumes and steel reinforcement. The walls' dimensions were 2.5 m in height, 2 m in length, designed with stiffeners and variable thickness, between 30-300 mm. These walls were tested by applying a distributed load to the wall stem through a spreader beam. All the UHPFRC walls exhibited displacement hardening behaviour after the first crack and failed due to a premature bond failure. Increasing the volumetric ratio of the steel fibres resulted in an increase in the wall toughness; however, the increase in the failure load was not noticeable.

Another study [17], tested a UHPC (without fibres) wall of size 1.5×2×0.05 m^3 placed over a traditional concrete slab, which posed an increased risk of cracking due to a high degree of restraint. The wall was reinforced with a Φ5mm steel mesh of mesh size 150 mm, positioned in the middle of the wall. This wall suffered the first crack two hours after formwork removal. This crack was the largest and after 120 days had a length of 850 mm and a width of 180 μm at the bottom of the wall, with decreasing width until 40 μm at the top of the crack.

UHPFRC has been effectively used in one of the ReSHEALience H2020 (Grant agreement ID: 760824) project pilots, which consists of water basins for collecting water from the cooling tower of a geothermal plant [18]. In that study, a traditional reinforced concrete solution (100 mm-thick cast-in-place) and two UHPFRC solutions were compared: a 60 mm-thick cast-in-place UHPC wall, and 30 mm-thin precast UHPC slabs supported by 200×200mm^2 cast-in-place UHPC buttresses. The best results were achieved in the two UHPFRC solutions, especially the precast solution with buttresses, in terms of steel fibre distribution, material consumption, and structural performance, and a healing index close to 80% was registered after being in contact with geothermal water.

The aim of this paper is to study the autogenous healing capability of two precast UPHFRC water reservoirs in which cracks were produced by autogenous shrinkage at an early-age, in order to investigate if self-healing may effectively close the cracks and recover the water tightness required for such structures.

2 Materials and methods

2.1 Description of the water reservoirs

In this study, two UHPFRC water reservoirs with internal dimensions of 1.30×0.75×0.70 m^3 were designed with the same geometric characteristics and materials. Both were produced in the laboratories of ICITECH, Universitat Politècnica de València (Spain).

The reservoirs were designed with a precast concept, where the elements were manufactured independently and subsequently assembled. Fig. 1 displays the elements of each of the water reservoirs, which consisted of: two frontal walls, two lateral walls, and one base. The frontal and lateral walls were assembled with bolted joints, displayed as small circles in the diagrams. The assembly process will be described in a later section.

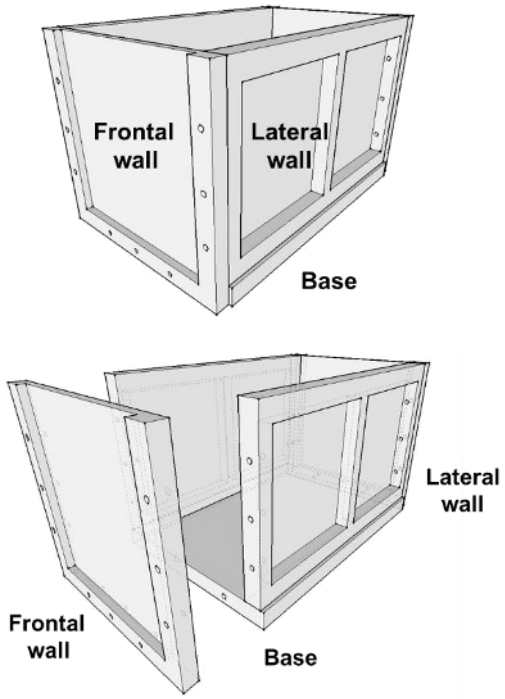

Fig. 1. 3D diagrams of the designed reservoirs indicating its elements.

The frontal and lateral walls were designed to have 30 mm thickness in the centre of the wall and the perimetral ribs had a section of 80×60 mm^2. The central area was unreinforced while the ribs were reinforced longitudinally with 2Ø6 rebars. The frontal walls do not have the top rib as displayed in Fig. 1.

The bases of the reservoirs were also ribbed, their central thickness was 30 mm, and their ribs had a section of 80×90 mm^2, and were reinforced longitudinally to the rib with 2Ø6 rebars.

The concept of these reservoirs is a very demanding design, using very small thickness to minimize the volume of concrete and without applying specific curing techniques, with the objective of analysing their risk of cracking by early-age shrinkage, the effects on watertightness and their self-healing potential to recover the required watertightness.

2.2 UHPFRC mix design

The concrete used to produce the reservoirs was a UHPFRC made with CEM I 42,5 R-SR 5 from Lafarge, two fine natural silica sands (0-0.4 mm and 0-1.6 mm), undensified silica fume from Elkem, and silica flour Quarzfin U-S 500 from Sibelco. The mix incorporated short straight-shaped steel fibres 13/0.2 (length 13 mm, Φ=0.2 mm, l_f/d_f = 13/0.2 = 65, tensile strength > 2000 MPa), to guarantee ductility and multiple micro-cracking. Sika® ViscoCrete®-20 HE was employed to obtain a self-compacting consistency. The water/cement (w/c) ratio of the mix was 0.2 and the water/binder ratio was 0.164. The mix composition is displayed in Table 1. Table 2 displays the properties of the fibres used.

Table 1. UHPFRC dosage used in this study.

Material	kg/m³
Cement	800
Silica Fume	175
Water	160
Fine Sand (0-0.4 mm)	565
Medium Sand (0-0.8 mm)	302
Silica Flour	225
Steel fibres	160
Superplasticizer	36

This mix had been thoroughly characterized in previous works. Its consistency in the slump flow test was a diameter of 680 mm. Regarding its mechanical properties, its average compression strength at 28d was 140 MPa, its tensile strength (f_t) was 9.5 MPa, and its ultimate tensile strength (f_{tu}) was 6.8 MPa with a strain value ε_{tu} of 2.36‰.

2.3 Mixing procedure

Four batches with volumes between 130 and 200 litres were produced for both water reservoirs using a P375T08 planetary concrete mixer.

The mixing procedure followed to produce the UHPFRC started with the introduction of aggregates, cement, silica fume, and silica flour into the mixer. Then, these materials were mixed for 1 min. Afterwards, 80% of the mixing water was added together with the superplasticizer and mixed for 15 min. After 15 min, the workability change of the mix had already been produced, and the fibres were introduced. Finally, the rest of the water was included in the mix and mixed for 5 additional min.

The mixes were poured into the wood formwork just after mixing. The formwork elements were removed one day after pouring. No specific curing was applied after formwork removal.

Table 2. Properties of the fibres.

Property	Steel fibres 13/0.2
Equivalent diameter (mm)	0.22
Length (mm)	13
Aspect ratio	59
Cross section shape	Round
Tensile strength (MPa)	≥2100
Image	

2.4 Casting and assembly

Firstly, frontal and lateral walls were cast independently for reservoir no.1 and reservoir no.2, and the bases were constructed afterwards.

The two lateral walls of reservoir no.1 were cast on 10th September 2020 (Fig 2), and on 18th September 2020, the two lateral walls of reservoir no.2 were cast. The four frontal walls (two per water reservoir) were cast on 14th September 2020 (Fig 3).

The slabs of both reservoirs were cast 11 days later, on 29th September 2020.

The self-compacting properties of this UHPFRC mix allowed casting all the ribs easily. Fig 3 shows the mix being poured into one of the formworks for a frontal wall.

Fig. 2. Formwork and placed rebars for the lateral walls

Fig. 3. Formwork of the lateral walls and UHPFRC being poured into the formwork of the frontal elements.

After this process, the formwork and reinforcement for the base elements were prepared. The frontal and lateral walls were placed in their final position. Frontal and lateral walls were fixed to one another by using threaded rods and nuts. Fig 2 shows these rod elements in the lateral walls' formwork and the holes prepared for the connection in the frontal walls' formwork (Fig 3). At this stage, the precast walls were around 10-14 days.

These frontal and lateral walls were connected to the base elements thanks to connecting rebars and the UHPFRC that formed the base. From the interior side, the joints between walls were sealed with epoxy resin adhesive mortar (MC© - SX 481 E). Between lateral and frontal walls, SikaSwell© water-stop was used, which is an expansive product used for systematic sealing in construction joints.

During the pouring process of the bases, clamps were used as an additional support for fixing the elements in their position. Additionally, plastic sheets were placed to ensure no leaks of UHPFRC were produced (see Fig 4). Fig. 5 shows the pouring process for producing the base of one of the reservoirs, which was done by pouring from the interior of the element, and thanks to its self-compacting properties, the material flowed and was distributed throughout the formwork.

Fig. 4. Frontal and lateral walls placed before pouring UHPFRC for the base of a reservoir.

Fig. 5. Pouring UHPFRC inside the formwork for producing the base of the reservoirs.

After the elements were cast, no cracks were visible in the two water reservoirs. The cracks studied in this work appeared when the reservoirs were filled with water.

2.5 Chronology of filling the water reservoirs and crack measurements

The two water reservoirs followed different chronologies of events regarding when they were put into operation. Once the two reservoirs were filled in with water, shrinkage cracks were completely visible in all the central areas of the walls and base. These cracks were passing cracks through the section of the wall. Cracks were not visible on the rib elements. Fig. 6 shows the two frontal walls from water reservoir no.1 with clear water leakage.

a) Chronology for water reservoir no.1:

On 28-10-2020, 29 days after casting the base element and assembly, reservoir no.1 was filled completely with water. Between 29-10-2020 at 14:30 and 30-10-2020 at 9:00, the level of water decreased by 20 mm, which is equivalent to 400 ml of leakage and evaporation.

One week later the reservoir was emptied (03-11-2020), and was kept empty until 11-11-2020, when it was filled again until the final measuring time on 10-12-2020, 43 days after the first contact with water.

b) Chronology for water reservoir no.2:

On 04-11-2020, 36 days after casting the base element and assembly, reservoir no.2 was filled completely with water. On 13-11-2021 (45 days after assembly), water temperature was increased until 60°C by means of two heat resistances. That temperature was achieved on 20-11-2020, one week later. Once 60°C was reached, it was maintained for one week, and on 28-11-2020, the resistances were shut down. Water reached ambient temperature in only two days. They were maintained at ambient temperature for the rest of the time of the test.

Finally, on the 13 and 14 of 01-2021, the reservoirs are emptied, and cracks from the bases were measured.
In order to analyze the self-healing performance, time 0 of healing is defined as the day when the reservoir is put in contact with water for the first time since water is the agent needed to promote the self-healing reactions. The chronology of filling the reservoirs with water and dates of crack measurements are displayed in Fig 6.

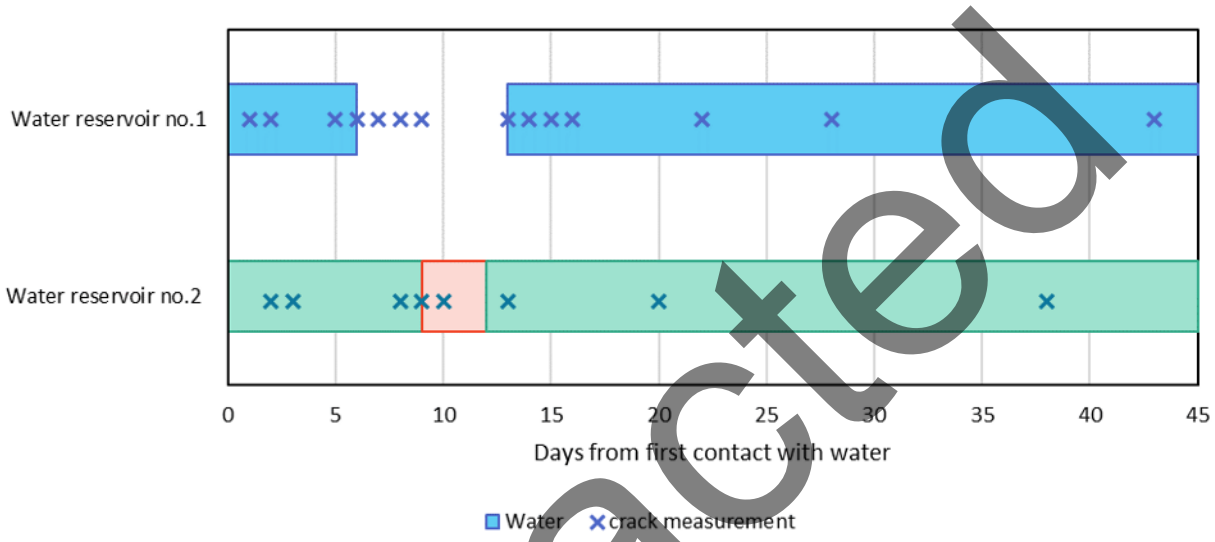

Fig. 6. Chronology of the presence of water in the reservoirs (bars) and crack measurements (crosses). The period of time without water in water reservoir no.1 is displayed as an empty area. The period of time with warm water in water reservoir no.2 is displayed in orange.

2.6 Crack measurement and self-healing evaluation

In order to evaluate the self-healing capability, the crack sizes on the two frontal walls of the two reservoirs were measured using a YINAMA Wi-Fi microscope. Among all the crack branches, the most representative cracks were chosen from those with apparent water leakage. Eight cracks from water reservoir no.1 were monitored (marked with circles and numbered in Fig 7) for 43 days. Four cracks from water reservoir no.2 were monitored for 37 days as well.

Lateral walls were not monitored because the surface irregularities made it difficult to obtain an accurate measure of the crack width. The base elements were not monitored during this period of time due to the accessibility restrictions and the cracks were only checked at the end of the monitoring period.

Furthermore, to have an accurate determination of the crack width on each point of analysis, three readings were taken. The average and maximum crack opening from these three readings were the parameters analysed. Besides, the healing performance of each point was evaluated using Eq. (1), using the initial crack width (at time 0 of healing) and the crack width measurement at time t.

$$Closing\ rate = 1 - \frac{Crack\ width\ at\ time\ t}{Initial\ crack\ width} \quad \text{(Eq. 1)}$$

3 Results and discussion

3.1 Cracking pattern and water leakage

Cracking was detected through visual observation when the reservoirs were filled with water and the cracks were wetted. Before this moment, cracks were not visible.

In all the walls, vertical and horizontal cracking was observed. Vertical cracks appeared in the walls and started at the confluence of the walls with the base, reaching 1/3 of the wall height. The highest cracks appeared in the middle of the wall. The horizontal cracks appear in the frontal walls. The crack patterns that were produced in the frontal walls of water reservoir no.1 are displayed in Fig 7. The crack pattern in water reservoir no.2 walls were very similar.

Fig. 7 Images of the two opposite frontal walls of reservoir no.1 with water leakage marks (top and bottom).

The average and maximum initial crack opening were measured in the frontal walls of the two reservoirs. These values are displayed in Fig 8 for the two reservoirs. All the cracks were below 100 µm (with the exception of one local reading), and the average value measured was generally below 50 µm. The low crack width values detected explains that cracks were not located before filling the reservoir with water, but they could have been present during the curing or assembly stages.

Cracks in the lateral walls and the bases were not monitored but the size of their cracks was also evaluated. All the cracks located in the lateral walls and bases were below 75 µm.

3.2 Crack width evolution and closing rate

Fig 9 shows the crack closing evolution of one representative crack of a frontal wall of water reservoir no.1. The photos show that after 7 days in contact with water cracks are partially filled with white deposits due to the self-healing reactions, and after 15 days the crack is visually filled completely. Surface deposits are also detected after 7 days, which are more present after 15 and 28 days of healing.

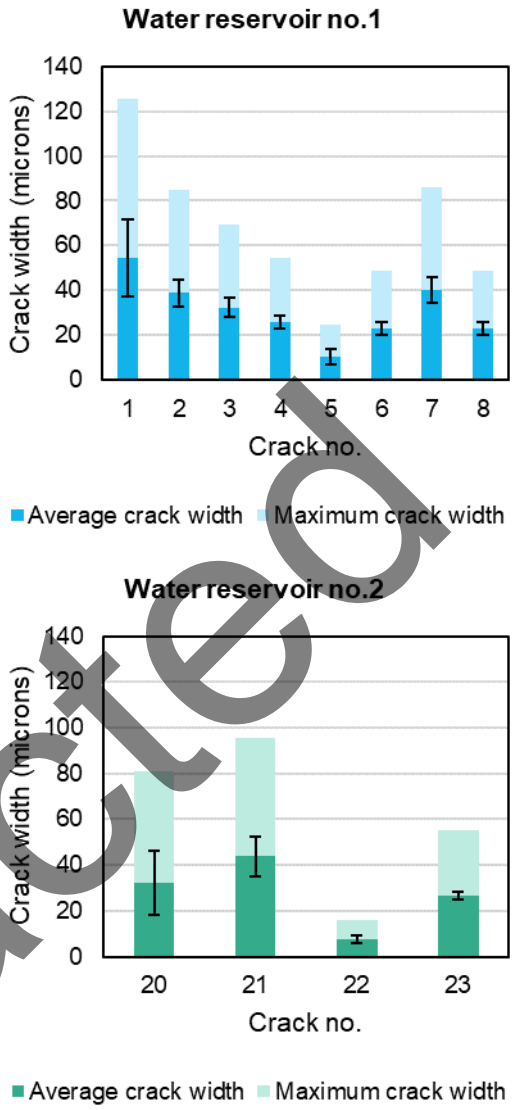

Fig. 8. Average and maximum crack width values were measured in the two water reservoirs before healing. Average values include standard deviation as the dispersion whiskers.

Before healing	After 7 days
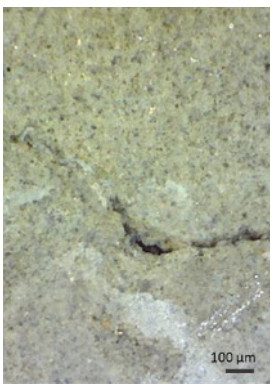	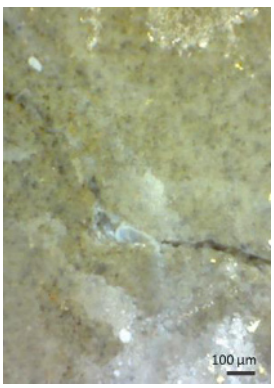

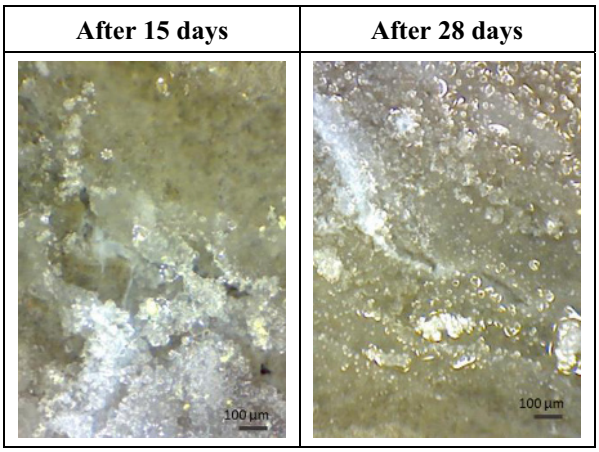

Fig. 9. Example of visual healing of a crack on the 1st, 7th, 15th, and 28th days after filling reservoir no.1 with water.

The crack width measurements on both reservoirs are presented in Fig 10 left column, where the horizontal axis indicates the number of days after filling the reservoir with water, which can be assimilated with the number of days from when effective healing can take place.

Fig 10 shows a linear descending trend for crack width in all the cracks on both reservoirs. Due to the small size of the cracks (usually lower than 80 µm), after 20 days of healing, almost all points of all the cracks were closed. As expected, larger cracks needed more time to be completely healed, while smaller cracks healed a few days after the first contact with water. Most of the process happened in the first week, which is consistent with the results from other studies [10], [19].

Additionally, the crack closing rate of each crack was evaluated using Eq. (1), and the values are displayed in Fig 10 right column, showing the gradual increase of the crack closing rate during the monitoring time. One crack had a slight reopening (negative closing rates), until day 9 of healing, followed by a full closing afterwards. Most of the cracks had complete closing after 20 days.

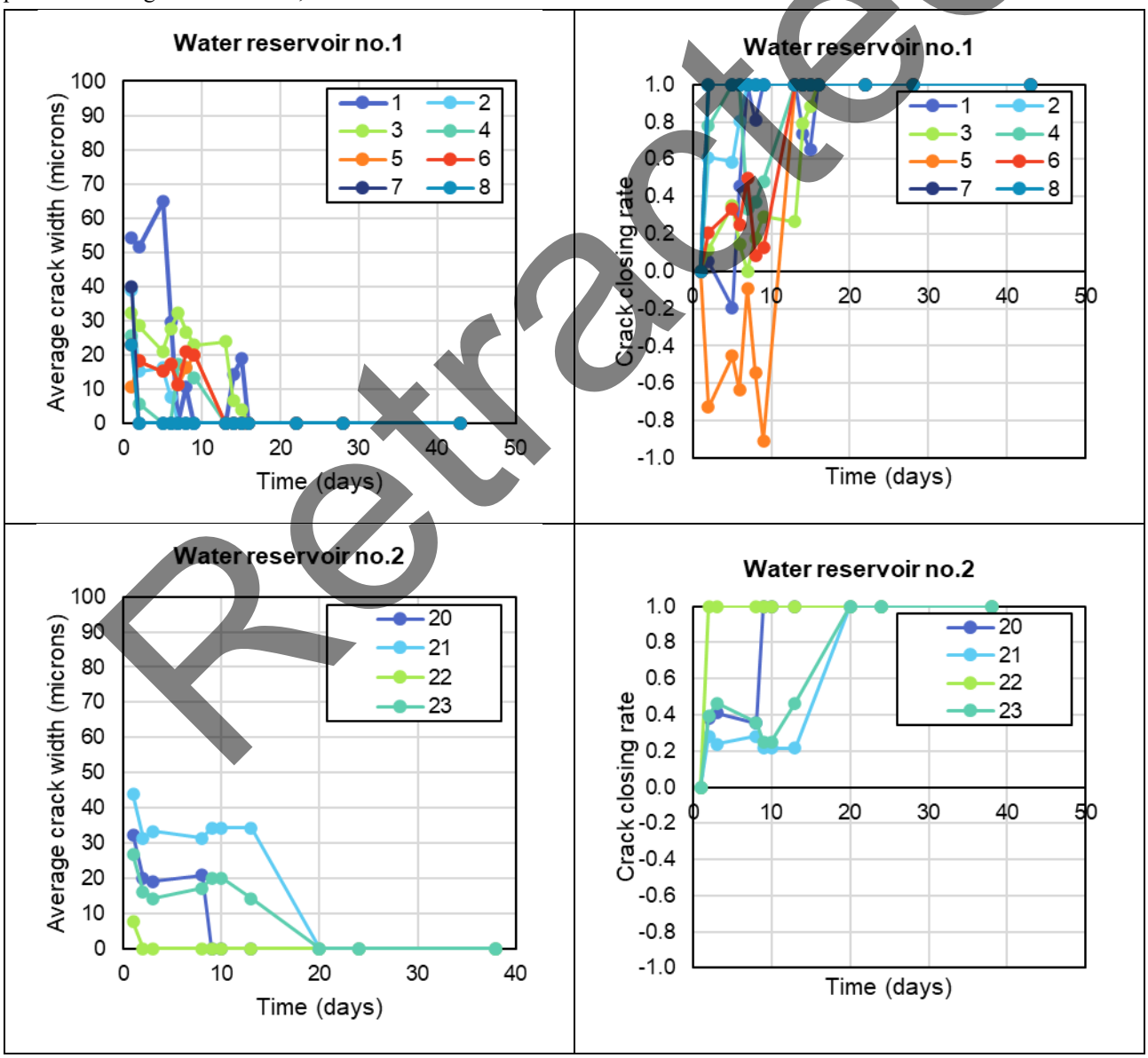

Fig. 10. Top row: Water reservoir no.1, bottom row: water reservoir no.2. Left column: crack width evolution. Right column: Crack closing rate of the cracks monitored.

3.3 Water tightness and discussion

The low amount of water leakage detected initially (21.6 ml/h ≈ 3.6×10^{-4} l/min) allowed the reservoirs to be operational despite the water loss, which could be feasible for some applications of reservoir structures. In any case, the water reservoirs stopped leaking water completely, which is consistent with published studies, where cracks as small as 17 µm have been reported to be practically watertight [19].

The concepts from EN1992-Part 3 for class 1 structures [2] can be applied to these reservoirs. In this case, the hydrostatic pressure (h_D) can be considered as 0.60 m, and the wall thickness of the containing structure (h) is 20 mm. The ratio h_D/h, in this case, is 600/20 = 30, which is an intermediate case of those indicated in the code. In this case, the value of crack width limit w_{k1} can be interpolated. Interpolating the values from the code, the limit for a crack width of these UHPFRC reservoirs that will experience an effective sealing would be around 75 µm, which is consistent with the results obtained.

4 Conclusions

This paper's purpose was to investigate in two water reservoirs whether the self-healing process was able to close the cracks visually and reduce water leakage recovering water tightness. The following conclusions can be drawn:

- UHPFRCs can ensure reduced crack width for early-age shrinkage cracking in thin elements. Vertical and horizontal cracks were detected in all the elements with reduced thickness. The walls of the water reservoirs had 20 mm thickness and all the passing cracks were under 80 µm.
- UHPFRC was able to heal autogenously, in direct contact with water, cracks under 80 µm in 20 days under a hydrostatic pressure of 600 mm, recovering completely the water tightness required for the water reservoirs, complying with the indications of EN1992-Part 3.

Acknowledgments

The authors would like to express their gratitude to the Spanish Ministry of Science, Innovation, and Universities for funding under the FPU Program [FPU18/06145].

The authors would also like to express their gratitude to Sika A.G. and MC Bauchemie for supplying materials used for this work.

References

1. C. Ryan, E. Garcia-Taengua, C. Chalioris, and E. Bastidas-Arteaga, *Sustain. 2021, Vol. 13, Page 11479*, **13**, 20, (2021)
2. *EUROPEAN STANDARD Eurocode 2-Design of concrete structures-Part 3: Liquid retaining and containment structures*. 1992.
3. M. Di Prisco, G. Plizzari, and L. Vandewalle, *Mater. Struct. Constr.*, **42**, 9, (2009)
4. T. E. T. Buttignol, J. L. A. O. Sousa, and T. N. Bittencourt, *Rev. IBRACON Estruturas e Mater.*, **10**, 4, (2017)
5. A. Mohebbi, B. Graybeal, M. Asce, and Z. Haber, *J. Mater. Civ. Eng.*, **34**, 6, (2022)
6. A. Loukili, A. Khelidj, and P. Richard, *Cem. Concr. Res.*, **29**, (1999).
7. A. Kamen, E. Denarié, H. Sadouki, and E. Brühwiler, *Cem. Concr. Res.*, **38**, 6, (2008)
8. F. A. Farhat, D. Nicolaides, A. Kanellopoulos, and B. L. Karihaloo, *Eng. Fract. Mech.*, **74**, 1–2, (2007)
9. V. Y. Garas, L. F. Kahn, and K. E. Kurtis, *Cem. Concr. Compos.*, **31**, 3, (2009)
10. J. P. Charron, E. Denarié, and E. Brühwiler, *Mater. Struct. 2006 403*, **40**, 3, (2006)
11. A. Martínez-Ibernón, M. Roig-Flores, J. Lliso-Ferrando, E. J. Mezquida-Alcaraz, M. Valcuende, and P. Serna, *Appl. Sci. 2020, Vol. 10, Page 239*, **10**, 1, (2019)
12. J. P. Charron, E. Denarié, and E. Brühwiler, *Cem. Concr. Res.*, **38**, 5, (2008)
13. D. Y. Yoo, W. Shin, B. Chun, and N. Banthia, *Cem. Concr. Res.*, **133**, (2020)
14. E. Cuenca and P. Serna, *Sustain.*, **13**, 6, (2021)
15. H. Doostkami, M. Roig-Flores, and P. Serna, *Constr. Build. Mater.*, **310**, (2021)
16. B. Nematollahi, Y. L. Voo, and R. Saifulnaz M. R, *KSCE J. Civ. Eng.*, **18**, 5, (2014)
17. J. Kheir *et al.*, *Eng. Fract. Mech.*, **257**, (2021)
18. S. Al Obaidi *et al.*, *Sustain.*, **13**, 17, (2021)
19. C.-M. Aldea, S. P. Shah, and A. Karr, **32**, (1999).

* Corresponding author: marcajor@upv.es